Supplementary Information

Thermotropic Phase Behaviour of Choline Soaps

Regina Klein,[a] Helen Dutton,[b] Olivier Diat,[c] Gordon J. T. Tiddy,[b] Werner Kunz[a]*

Table of Content

I. Thermogravimetric analyses

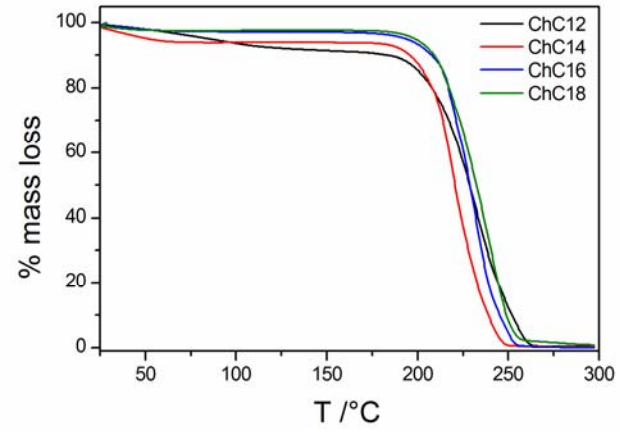

Figure 1. TGA curves of ChC*m* surfactants for *m*= 12-18.

All investigated choline soaps show a one-step degradation process. The initial decay of ChC12 and ChC14 arises most probably from evaporating water.

II. DSC diagrams

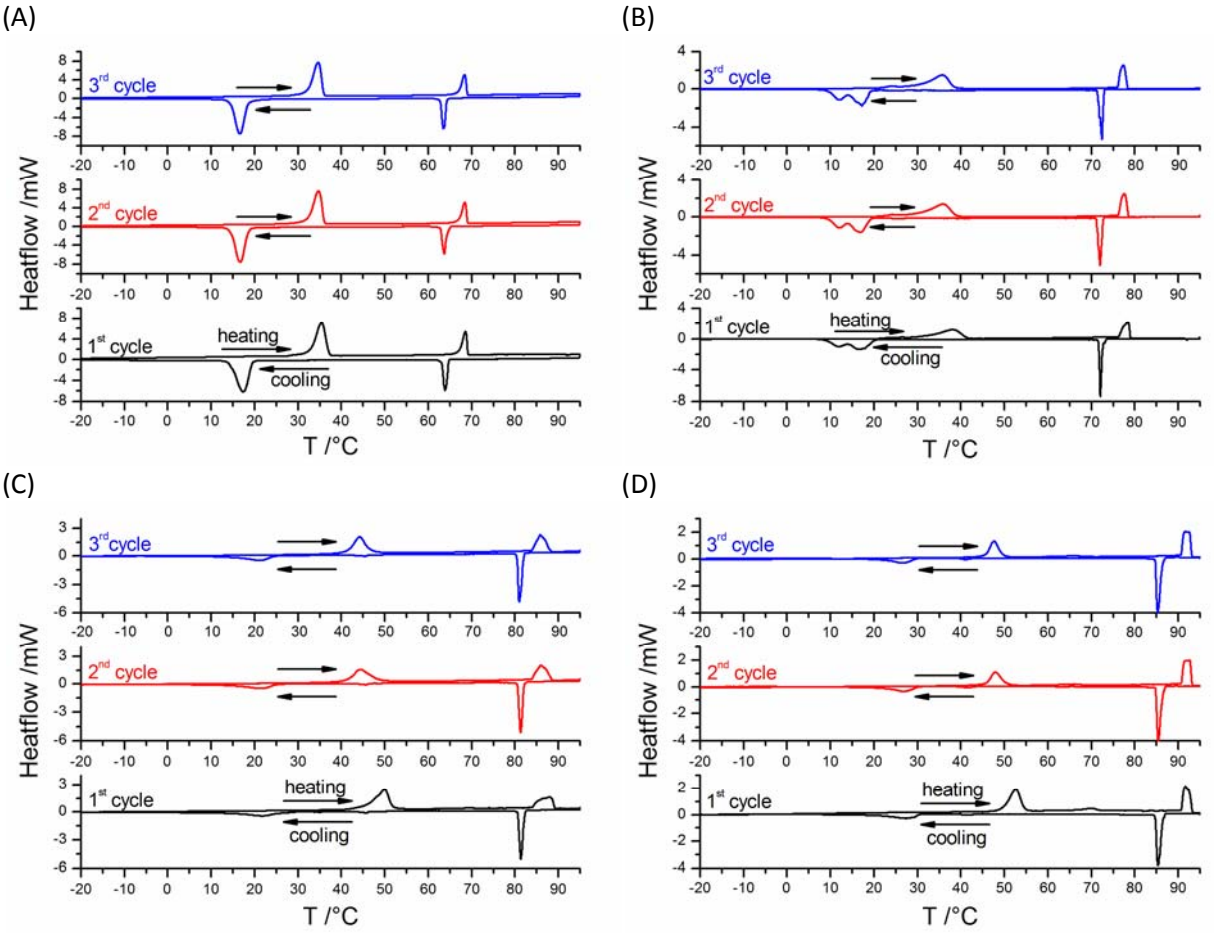

Figure 2. Three DSC cycles of ChC*m* surfactants between -20°C and 95°C: *m*= 12 (A), *m*= 14 (B), *m*= 16 (C) and *m*= 18 (D).

III. Transition temperatures

In the following, the index “1” mark the low-temperature transitions and “2” the high-temperature ones.

	ChC12		ChC14		ChC16		ChC18	
	T_1 /°C	T_2 /°C	T_1 /°C	T_2 /°C	T_1 /°C	T_2 /°C	T_1 /°C	T_2 /°C
1st heating	35.4	68.6	38.1	78.4	50.0	87.9	52.6	91.6
1st cooling	17.3	63.9	16.5	72.1	21.4	81.4	27.4	85.4
2nd heating	34.7	68.4	36.0	77.6	44.4	85.9	47.9	92.6
2nd cooling	16.7	63.7	16.9	72.0	21.2	81.3	26.9	85.4
3rd heating	34.6	68.4	35.7	77.4	44.2	85.8	47.6	92.5
3rd cooling	16.6	63.5	17.2	72.5	21.3	81.0	26.7	85.3

Table 1. Transition temperatures on heating and cooling of ChC*m* surfactants for *m*= 12-18 as determined by DSC for three cycles between -20°C and 95°C.

IV. Transition enthalpies

	ChC12		ChC14		ChC16		ChC18	
	ΔH_1 /kJ mol^{-1}	ΔH_2 /kJ mol^{-1}	ΔH_1 /kJ mol^{-1}	ΔH_2 /kJ mol^{-1}	ΔH_1 /kJ mol^{-1}	ΔH_2 /kJ mol^{-1}	ΔH_1 /kJ mol^{-1}	ΔH_2 /kJ mol^{-1}
1st heating	28.3	9.2	23.4	12.9	26.7	14.2	25.5	15.9
1st cooling	-27.7	-9.1	-22.9	-13.0	-17.9	-15.3	-14.4	-19.5
2nd heating	28.1	9.0	24.2	12.0	21.9	14.7	19.2	16.8
2nd cooling	-27.6	-9.0	-22.5	-12.0	-17.7	-15.2	-14.6	-19.4
3rd heating	27.2	9.1	24.4	12.2	19.7	15.2	21.2	16.8
3rd cooling	-27.9	-9.0	-22.7	-12.3	-17.9	-15.1	-14.3	-19.5

Table 2. Transition enthalpies on heating and cooling of ChC*m* surfactants for *m*= 12-18 as determined by DSC for three cycles between -20°C and 95°C.

	ChC12	ChC14	ChC16	ChC18
	∑H /kJ mol^{-1}	∑H /kJ mol^{-1}	∑H /kJ mol^{-1}	∑H /kJ mol^{-1}
1st heating	37.5	36.3	40.9	41.4
1st cooling	-36.8	-35.9	-33.2	-33.9
2nd heating	37.1	36.2	36.6	36.0
2nd cooling	-36.6	-34.5	-32.9	-34
3rd heating	36.3	36.6	34.9	38.0
3rd cooling	-36.9	-35.0	-33.0	-33.8

Table 3. Sum of the transition enthalpies of ChC*m* surfactants for *m*= 12-18 as obtained by DSC for three heating-cooling cycles between -20°C and 95°C.

V. Optical polarizing microscopy

All pictures were recorded at 100x magnification with a heating and cooling rate of 10°C min^{-1}. The photographs presented in the following were taken at the first cooling cycle. The light intensity and the sample position were kept constant.

V.1. ChC14

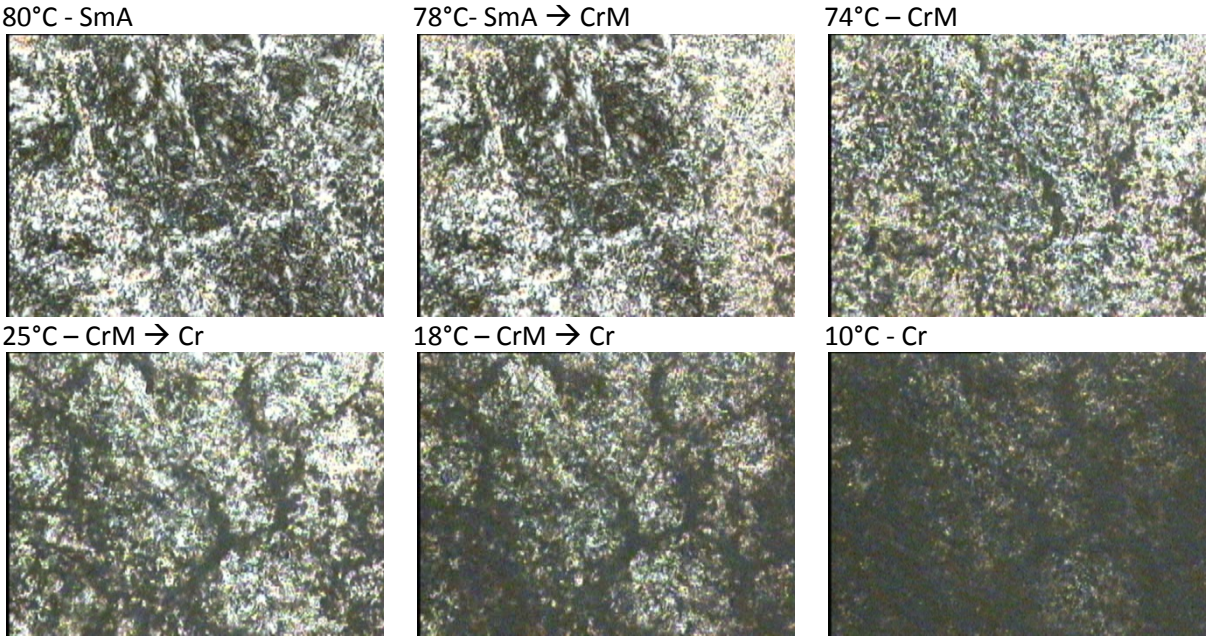

Figure 3. Polarizing microscopy images of ChC14 obtained on the first cooling between 100°C and -20°C. Above 78°C a low viscous liquid-crystalline lamellar phase (SmA) is present. At 78°C - 75°C, the transition from SmA to a semi-crystalline (CrM) phase takes place, which is obvious by a sudden increase of viscosity and change of texture. On further cooling, the appearance of the sample changes gradually and breaks in the texture indicate a stepwise increment of density. Between 25°C and 10°C, the sample turns finally completely dark, corresponding to the transition from CrM to crystalline (Cr).

V.2. ChC16

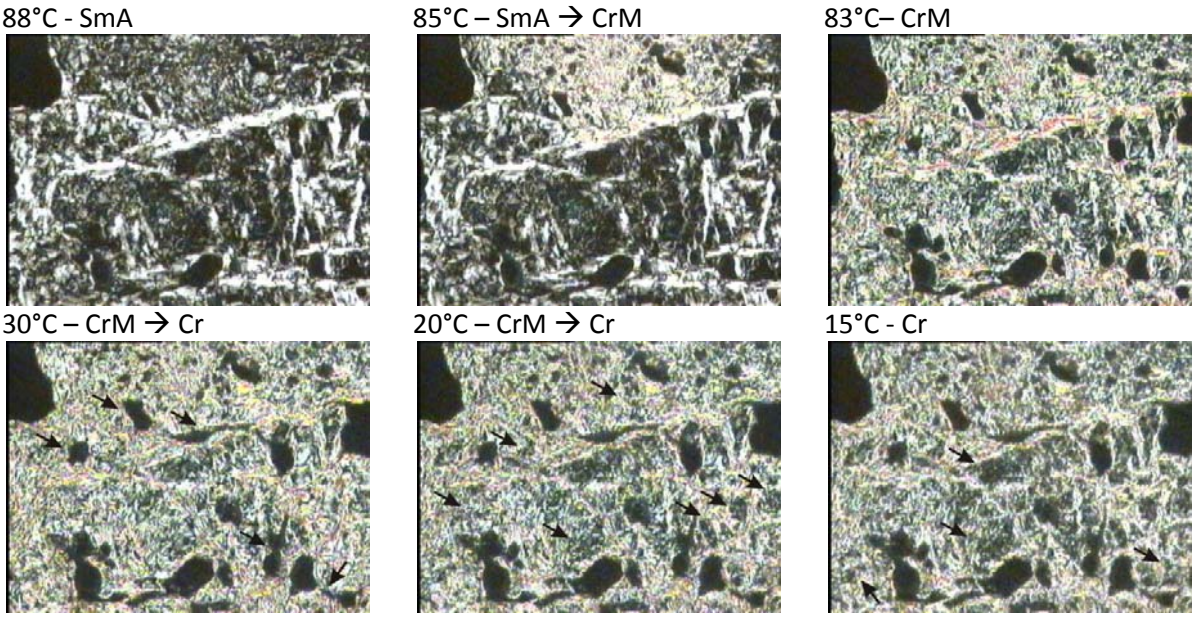

Figure 4. Polarizing microscopy images of ChC16 obtained on the first cooling between 100°C and -20°C. At high temperatures (> 86°C), a liquid-crystalline lamellar phase can be identified by its characteristic oily streak texture and low viscosity. At 85°C - 83°C, the sample gets abruptly highly viscous and birefringent, which corresponds to the transition from SmA to a semi-crystalline (CrM) phase. On further cooling, breaks in the texture (as assigned b the arrows) gradually appears, indicating a growing density. The transition from CrM to crystalline (Cr) between 20°C and 15°C gets obvious from an attenuation of birefringence and a sudden increment of the breaks in the texture. This texture remains constant down to -20°C.

V.3. ChC18

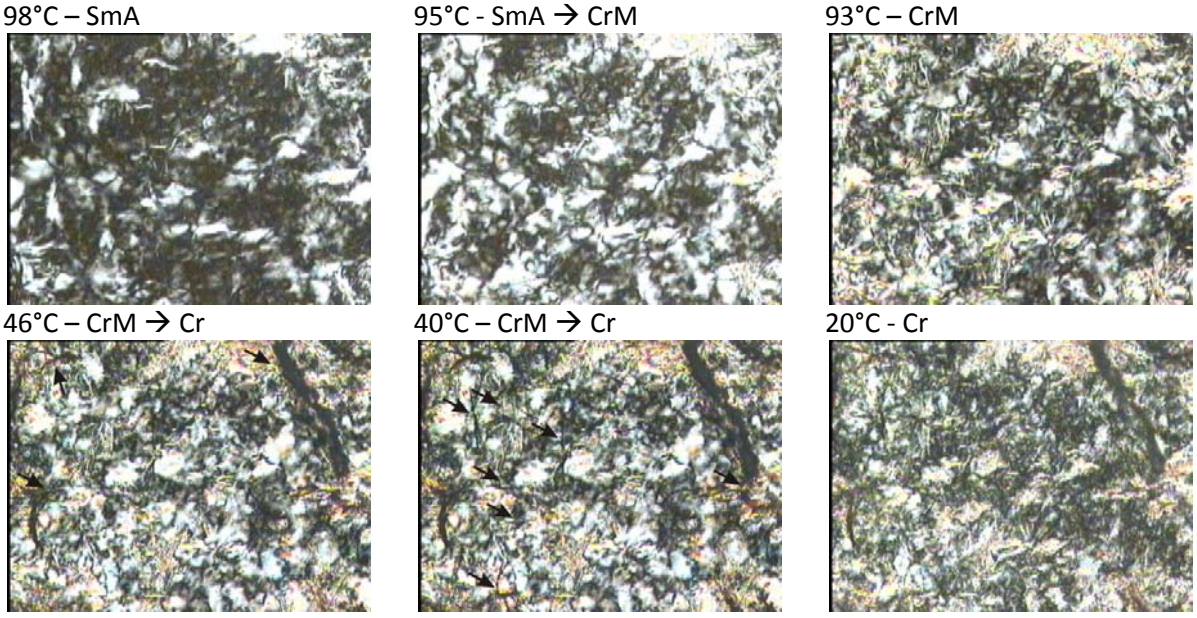

Figure 5. Polarizing microscopy images of ChC18 obtained on the first cooling between 100°C and -20°C. At high temperatures (> 96°C), a liquid-crystalline lamellar phase can be identified its characteristic oily streak texture and low viscosity. At 95°C - 93°C, the sample gets rapidly highly viscous and birefringent, which corresponds to the transition from SmA to semi-crystalline (CrM) phase. On further cooling, the appearance of the sample changes gradually, accompanied with breaks in the texture (as assigned by the arrows). The transition from CrM to crystalline (Cr) between 46°C and 35°C gets obvious from an attenuation of birefringence and a sudden increment of the breaks in the texture. Once Cr is formed, the appearance of the sample remains constant down to -20°C.

VI. NMR proton spin-spin relaxation times T_2

		ChC12	ChC14	ChC16	ChC18
	T /°C	T_{2eff} /µs	T_{2eff} /µs	T_{2eff} /µs	T_{2eff} /µs
heating	10.9	4	3.5	4	3
	20.6	4	-	-	-
	25.5	-	4	4.5	3
	30.1	5	-	-	-
	39.3	23	7.5 - 2Φ (?)	5.5	3
	48.6	29	-	-	-
	53.2	-	27	26.5	17.5
	57.9	28	-	-	-
	67.4	31.5	28	34 - 2Φ	19
	77.0	115	-	-	-
	81.8	-	125	52	24 - 2Φ (≈ 5%)
	91.4	165	-	-	-
cooling	67.4	-	29	36.5 - 2Φ	24.5 - 2Φ (< 1%)
	57.9	30.5	-	-	-
	53.2	-	28	31.5	23.5
	39.3	29.5	26.5	25	21.1
	25.5	21	18.5 - 2Φ (?)	20.5	9
	11.5	4.5	4.5	10 - 2Φ (?)-	-
	10.9	-	-	-	6
Intensity at 1/e		3.13	2.68	2.57	2.68

Table 4. NMR proton spin-spin relaxation constants T_{2eff} of ChC*m* surfactants (*m*= 12-18) as a function of temperature.

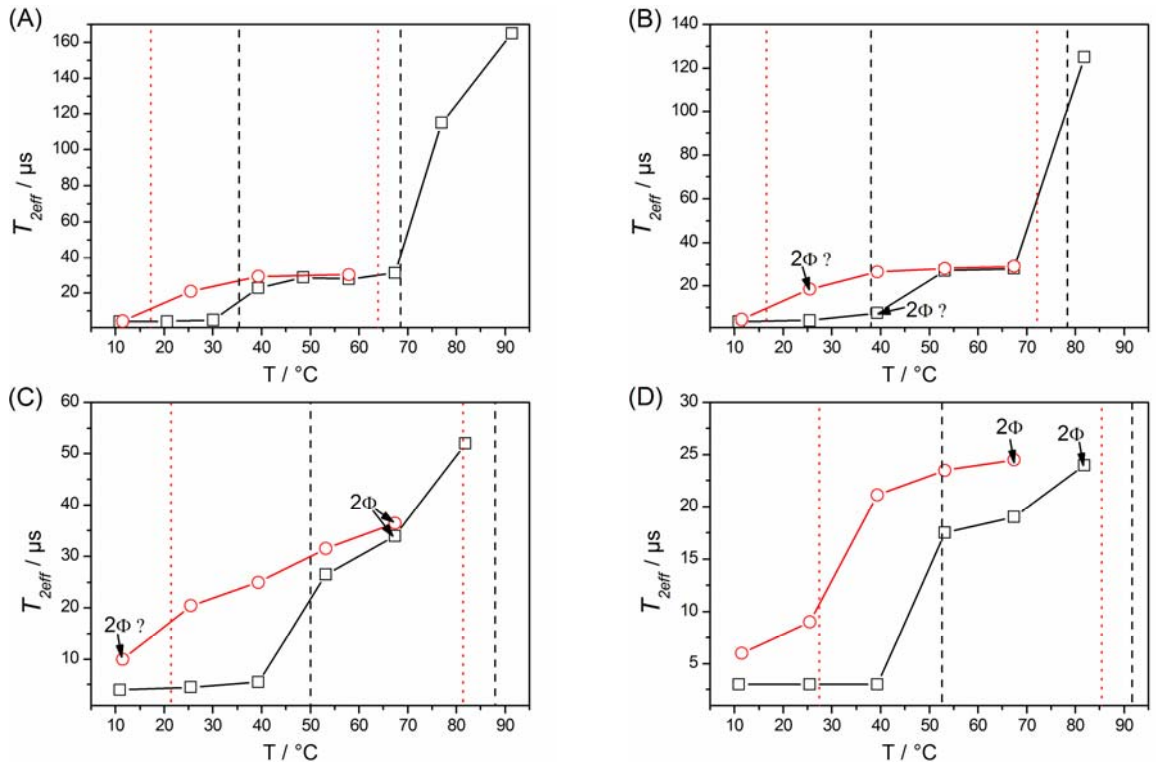

Figure 6. Variation of the decay constant T_2 with temperature ((□) heating, (○) cooling) of ChC*m* surfactants for *m*=12 (A), *m*=14 (B), *m*=16 (C) and *m*=18 (D). The black dashed vertical lines mark the transition temperatures on heating as detected by DSC, and the dotted red ones those on cooling (both for the first cycle).

VII. X-ray scattering curves of ChC*m* soaps as a function of temperature

VII.1. ChC12

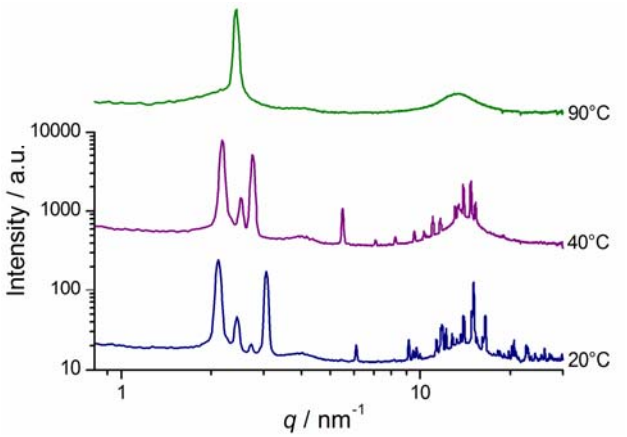

Figure 7. Small- and wide-angle X-ray scattering curves of neat ChC12 on raising temperature (freshly melted sample).

VII.2. ChC14

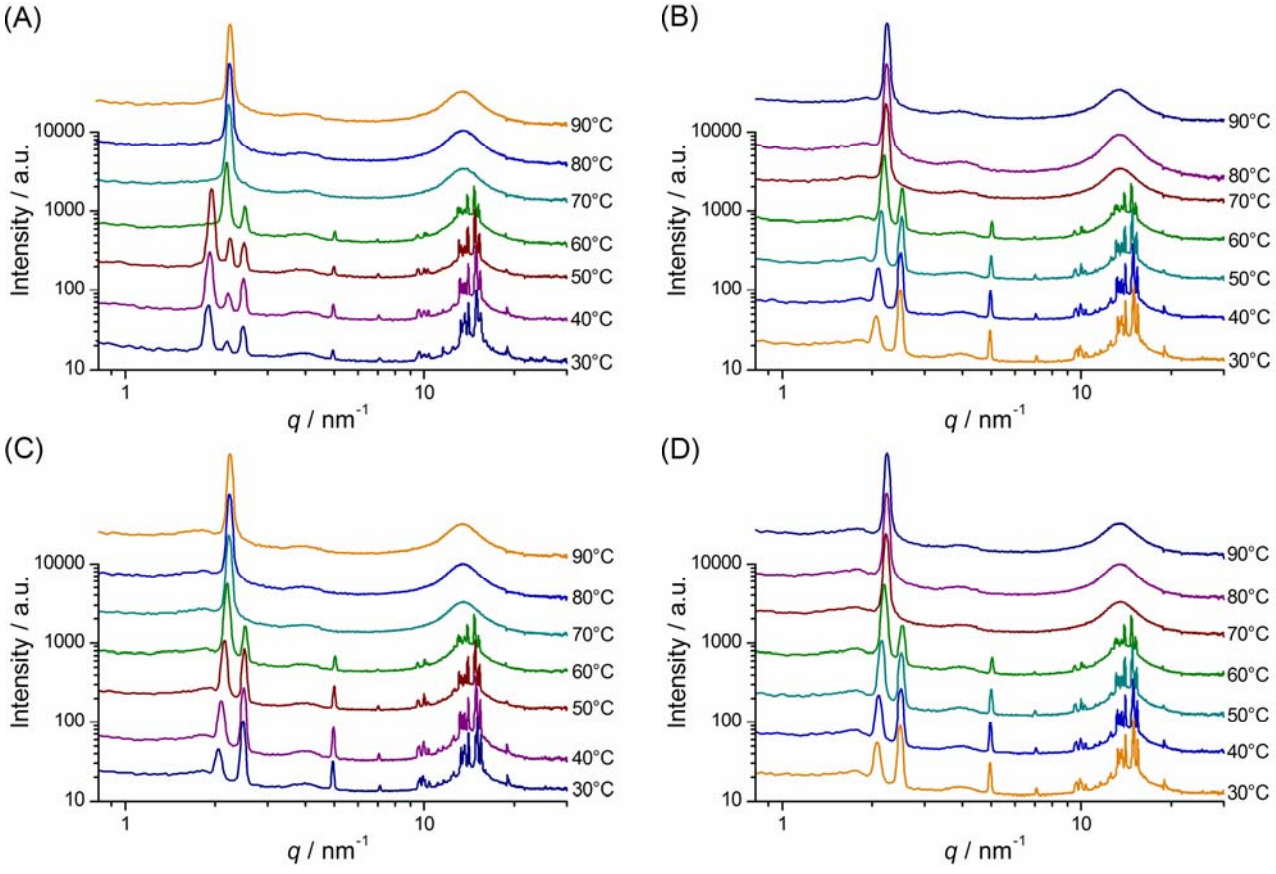

Figure 8. Small- and wide-angle X-ray scattering curves of neat ChC14 at various temperatures and heating-cooling cycles: (A) freshly heated, (B) first cooling, (C) re-heated and (D) second cooling.

VII.3. ChC16

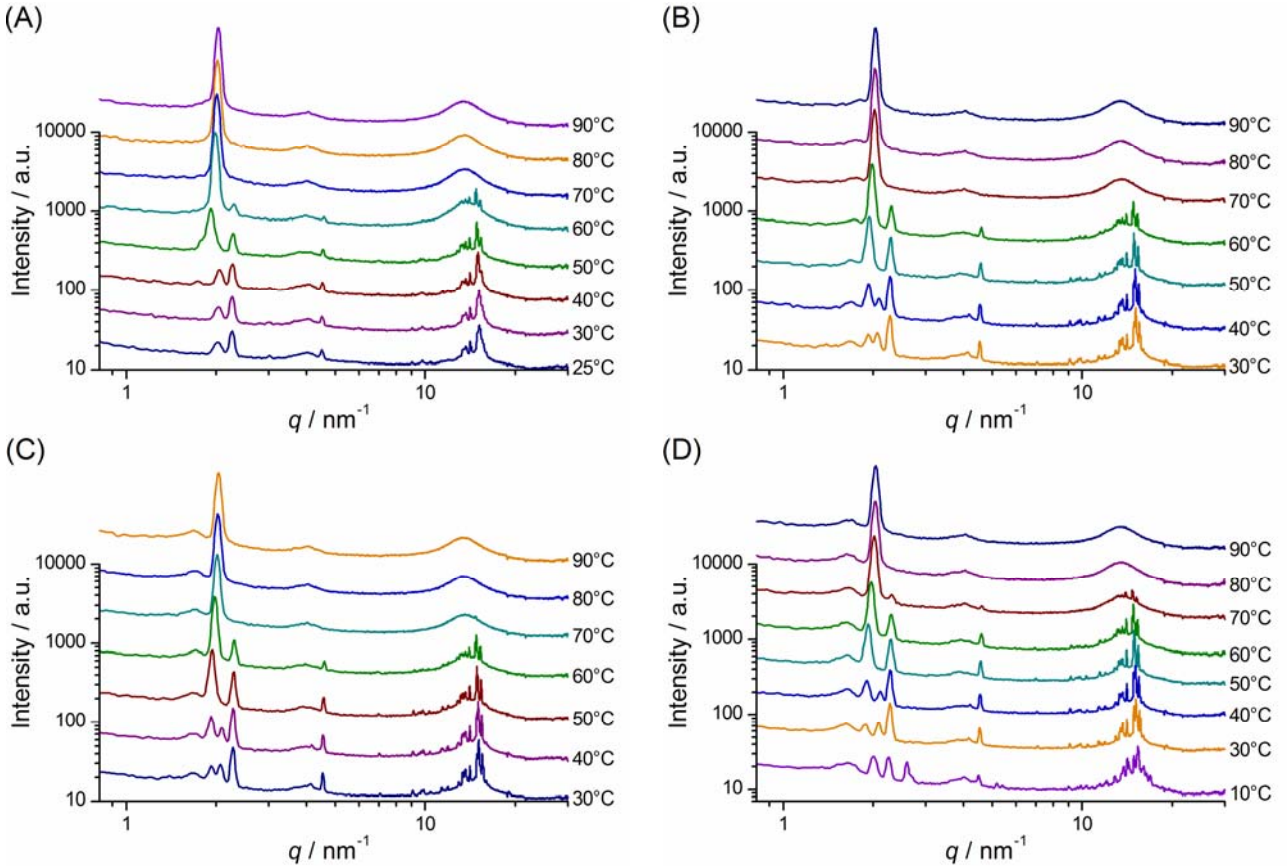

Figure 9. Small- and wide-angle X-ray scattering curves of neat ChC16 at various temperatures and heating-cooling cycles: (A) freshly heated, (B) first cooling, (C) re-heated and (D) second cooling.

VII.4. *d*- spacing of ChC*m* surfactants as a function of temperature

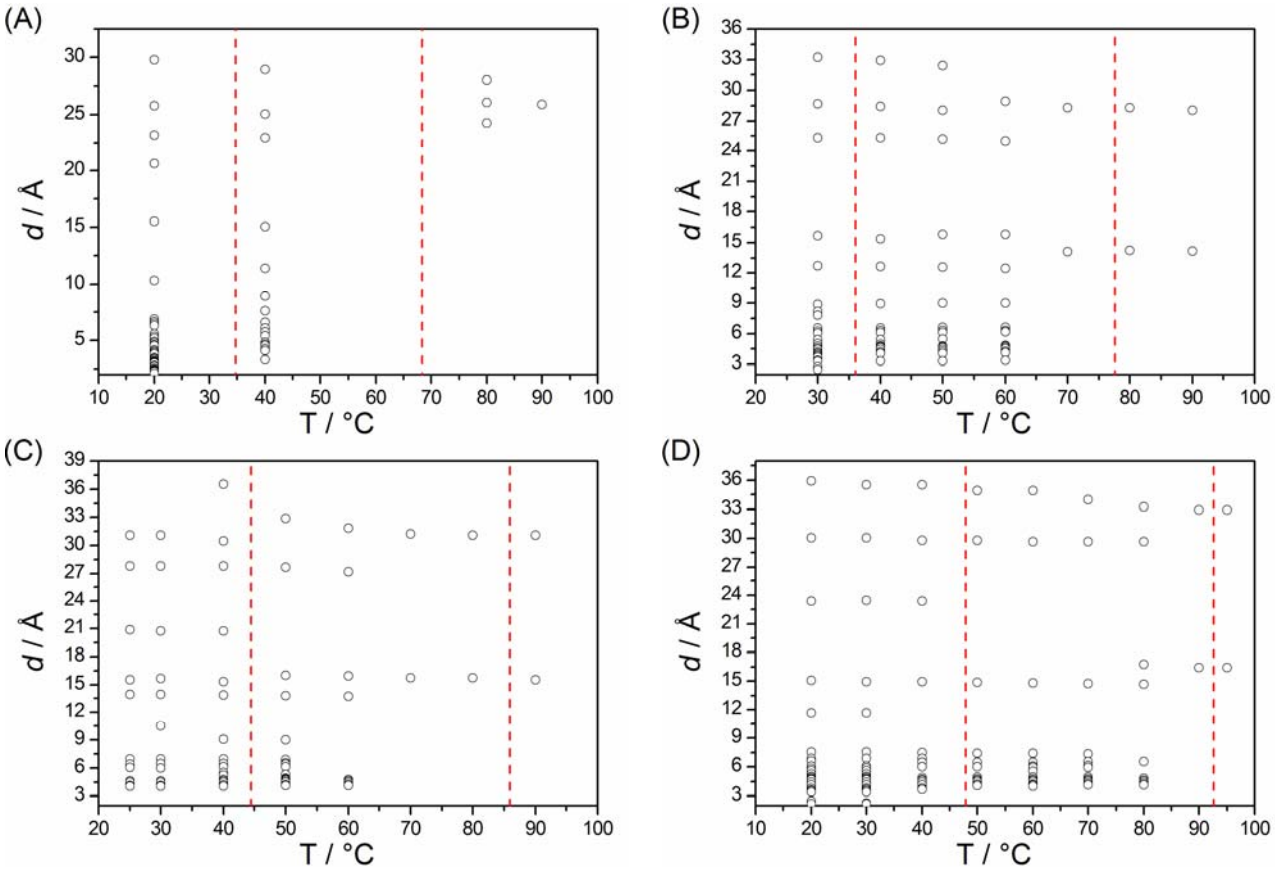

Figure 10. Evolution of the d-spacing values of neat ChC*m* surfactants with raising temperature (freshly melted samples): *m*= 12 (A), *m*= 14 (B), *m*= 16 (C) and *m*= 18 (D). The vertical dashed red lines mark the transition temperatures determined by DSC.

VII.5. *d*- spacing of ChC*m* surfactants as a function of *m* at low temperatures

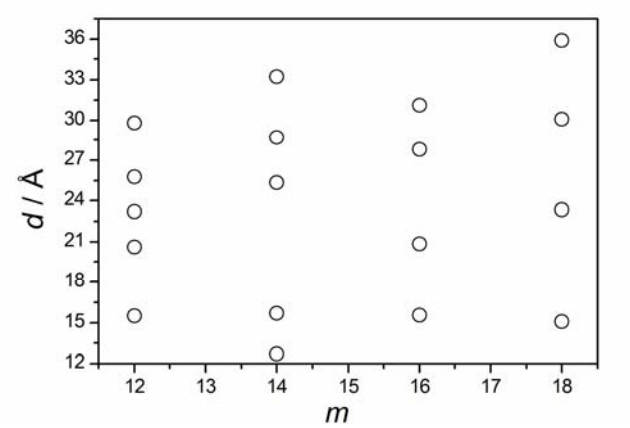

Figure 11. Comparison of the low-angle *d*-spacing values (up to *q*= 5 nm^{-1}) for different alkyl chain lengths (*m*= 12-18) at low temperatures (20°C for *m*= 12 and 18, 25°C for *m*= 16, and 30°C for *m*= 14).

VII.6. *d*- spacing of ChC*m* surfactants as a function of *m* at 40°C

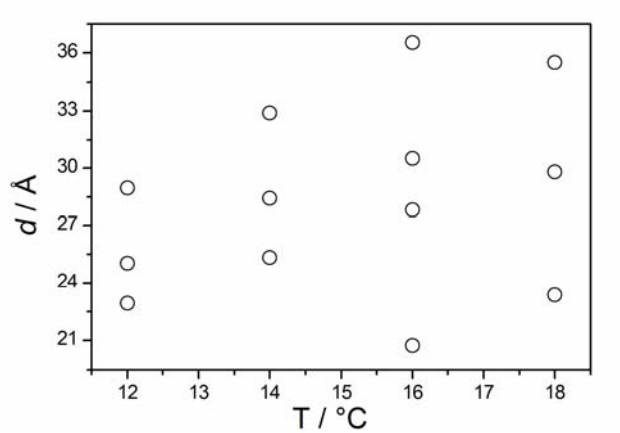

Figure 12. Comparison of the low-angle *d*-spacing values (up to *q*= 5 nm^{-1}) for *m*= 12-18 at 40°C.